NJC

PAPER

Preparation and characterization of colloidal copper xanthate nanoparticles†

Yuri Mikhlin,*[a] Sergey Vorobyev,[ab] Svetlana Saikova,[b] Yevgeny Tomashevich,[a] Olga Fetisova,[a] Svetlana Kozlova[a] and Sergey Zharkov[bc]

Despite the important role of metal xanthates in a number of industrial processes and emerging applications, no attempts have been made to prepare the metal xanthate nanoparticles and to study colloidal solutions of insoluble heavy metal xanthates. Here, we examined the formation of colloidal copper xanthate particles during the reactions of aqueous solutions of cupric sulfate and various potassium xanthates, which occur in flotation and water treatment slurries and can be used to manufacture nanoparticles for materials science (*e.g.,* as precursors for copper sulfide nanoparticles and biomedicine). The products were characterized using UV-vis absorption, dynamic light scattering, zeta potential measurements, transmission electron microscopy (TEM), electron diffraction, Fourier transform infrared spectroscopy, thermogravimetry, X-ray photoelectron spectroscopy, and X-ray absorption spectroscopy (XANES). Colloidal copper xanthates with compositions of ROCSSCu (R = ethyl, isopropyl, butyl, isobutyl, and amyl groups), disordered structures and average diameters of 20–80 nm easily formed and aggregated and were stable for at least several hours, especially if excessive xanthate was used. The hydrodynamic diameters of the nanoparticles were smaller at lower temperatures. Dixanthogens, which were produced in the reactions along with ROCSSCu, seemed to promote nanoparticle aggregation and precipitated with the copper xanthate, affecting their thermal decomposition. The TEM micrographs and S K- and Cu K-edge XANES spectra revealed core/shell particle morphologies, likely with Cu(I) bonded to four S atoms in the core and reduced copper coordination in the shell.

Introduction

Metal xanthates, salts of the O-esters of carbonodithioic acids and the corresponding O,S-diesters ROCSSH, where R stands for an alkyl chain (ethyl-, propyl-, butyl-, *etc.*), are widely used as collectors in the froth flotation of metal sulfide ores, as reagents for heavy metal sedimentation in hydrometallurgy and wastewater treatment, in cellulose synthesis, as vulcanization accelerators in rubber industry, and in other applications.[1–9] Cytotoxic activity of metal xanthates on human cancer cells has been found;[10,11] however, the testing of some compounds including copper xanthates has been hindered by their low solubility.[11] In materials science and nanotechnology, xanthates have been proposed as capping agents for the synthesis of metal nanoparticles and self-assembled monolayers as alternatives to thiols and as sulfidizing reagents for the preparation of metal sulfide nanoparticles.[12–15] The interest in metal xanthates as precursors of metal sulfide nanostructures has rapidly grown in recent years since their low decomposition temperatures make them compatible with organic polymers for the manufacturing of hybrid photovoltaic devices.[15–19]

The structures and properties of bulk metal xanthates, including copper xanthates, along with related substances and their soluble and adsorbed species have been reported in a number of studies (see, in particular ref. 3, 4, 6, 11 and 20–32). It is well known that the direct interaction of aqueous Cu^{2+} cations with xanthate ions yields a yellow precipitate of ROCS(S)Cu and dialkyl dixanthogen:[20]

$$4ROCSSK + 2CuSO_4 = (ROCSS)_2 + 2ROCSSCu$$
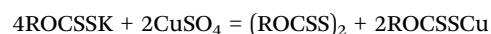
However, to the best of our knowledge, no studies have been aimed at the formation of the nanoparticles and colloids of xanthates of copper or other metals, which could be potentially used as carriers for poorly water-soluble metal xanthates in several applications, including flotation, biomedicine, and materials science. This research is also important for understanding the behavior and role of aquatic metal xanthate nanoparticles that are formed, intentionally or unintentionally, in the flotation slurries, tail dumps and wastewaters of concentrating mills and water treatment systems. It is worth noting that the

[a] *Institute of Chemistry and Chemical Technology of the Siberian Branch of the Russian Academy of Sciences, Akademgorodok, 50/24, Krasnoyarsk, 660036, Russia. E-mail: yumikh@icct.ru*
[b] *Siberian Federal University, Svobodny pr. 79, Krasnoyarsk, 660041, Russia*
[c] *Kirensky Institute of Physics of the Siberian Branch of the Russian Academy of Sciences, Akademgorodok 50/38, Krasnoyarsk, 660036, Russia*
† Electronic supplementary information (ESI) available. See DOI: 10.1039/c6nj00098c

preparation of metal xanthate nanoparticles, especially for large-scale mineral processing and water treatment, should be easy and cost-effective.

In the current paper, we describe the formation of colloidal copper xanthate particles *via* the simple mixing of aqueous solutions of cupric sulfate and various potassium xanthates. We demonstrated that the particles having ROCSSCu compositions with admixtures of dixanthogen and core/shell structures are largely amorphous, and their sizes and aggregative stability depend mainly upon the initial ratio of the reactants and temperature, although the nature of the alkyl groups is also important.

Experimental

Materials and preparation

Commercial reagents potassium ethyl xanthate (CH_3CH_2OCSSK), isopropyl xanthate ($C_2H_6CHOCSSK$), *n*-butyl xanthate and isobutyl xanthate ($C_3H_7CH_2OCSSK$), and amyl xanthate ($C_4H_9CH_2OSSK$; about 95% purity, purchased from Volzhsky Orgsynthese, JSC) were recrystallized two times in acetone and kept frozen. Fresh solutions of these reagents were prepared directly using doubly distilled water before synthesis. Other chemicals were of analytical grade and were used as received. In a typical experiment for the synthesis of copper xanthate, 1 mL of $CuSO_4$ solution (3 mM) and 1 mL of potassium xanthate solution (concentration varied from 0.15 mM to 12 mM to obtain a predetermined Cu-to-xanthate ratio) were added to 1 mL of water and agitated for 5 min at a desirable temperature (pH $\sim$ 8); the reaction mixture became yellow in several seconds. The solution was then loaded into a cell for UV-vis absorption spectroscopy, dynamic light scattering (DLS), or zeta potential measurements. The copper xanthate samples for spectroscopic examination using Fourier transform infrared spectroscopy (FTIR), X-ray photoelectron spectroscopy (XPS) and X-ray absorption spectroscopy along with samples for thermogravimetric analysis (TGA) were precipitated from the 1 mM colloidal solutions or from more concentrated solutions with the same reagent ratios by centrifugation at $10 \times g$ for 20 min, washed with water by decantation, and dried in air. Some samples were washed with acetone in order to remove dixanthogen.

Characterization

UV-vis absorption spectra were collected using an Evolution 300 instrument (Thermo Scientific) in a thermostatic 1 cm quartz cell; when necessary, the solutions were diluted with water. DLS and zeta potential studies were conducted using a Zetasizer Nano ZS spectrometer (Malvern Instruments Ltd, UK) with a scattering angle of 173° at the desired temperature in a folded polystyrene cell or polycarbonate cell with Pd electrodes. The volume-weighted mean size (Z_{av}) was typically considered in this study due to its high reliability. Transmission electron microscopy (TEM) experiments were performed with a JEM-2100 microscope (JEOL) operating at 200 kV. Samples were prepared by placing a hydrosol droplet on a carbon-coated copper grid and allowing the solvent to evaporate at room temperature. FTIR spectra were recorded on a Bruker Vector 22 Fourier spectrometer

using KBr pellets. Thermogravimetric (TG) and differential thermal analysis from ambient temperature to 900 °C were performed using an STA449 F1 Jupiter instrument (Netzsch) with a heating rate of 10 °C min^{-1} in air or argon at a gas flow rate of 50 mL min^{-1}.

XPS spectra were collected from the precipitate attached to a conducting carbon tape with a SPECS instrument equipped with a PHOIBOS 150 MCD 9 hemispherical analyzer at an electron take-off angle 90°. Monochromatized Al Kα excitation (1486.6 eV) was used, and the analytical chamber pressure was in the range of 10^{-9} mBar. The binding energies were corrected using the C 1s reference (285.0 eV) from aliphatic carbon. A low-energy electron flood gun was employed to eliminate the inhomogeneous electrostatic charging of the samples. The spectra were fitted using Gaussian–Lorentzian peak profiles after Shirley background subtraction with CasaXPS software.

Cu K-edge and S K-edge X-ray absorption spectra were acquired at the HIKE endstation located at the BESSY KMC-1 beamline (Helmholtz Zentrum Berlin). Total electron yield (TEY) and partial fluorescence yield (FY) modes were used simultaneously, and an Si(111) crystal served as the monochromator. The measurements were carried out in a UHV chamber with a vacuum better than 1×10^{-8} mBar at room temperature.

Results and discussion

UV-vis spectroscopy

The reaction systems contained 1 mM $CuSO_4$ and variable concentrations of different potassium xanthates to achieve predetermined xanthate-to-Cu ratios. The reaction mixtures became yellow in several seconds; this is commonly believed to indicate the formation of copper xanthate hydrosols since the solubility product of copper ethyl xanthate is as low as 5.2×10^{-20} and decreases with increasing alkyl chain length to 8×10^{-22} for copper amyl xanthate.[22,23] Fig. 1 shows the typical electronic absorption spectra of the initial xanthate solutions and the reaction media. The spectrum of xanthate displays absorption maxima at 227 nm (A) and 300 nm (C), which should be assigned to the n–σ* electron transition of the C=S group and the π–π* transition of the O–C–(S)S moieties,[20,30,31] respectively. These maxima decreased or disappeared, depending on the
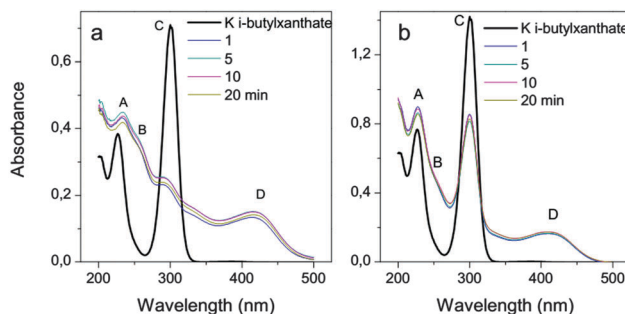

Fig. 1 UV-vis absorption spectra of potassium isobutyl xanthate and the reaction solutions with xanthate-to-copper sulfate molar ratios of (a) 1.5 : 1 and (b) 3 : 1 for varying reaction times at 30 °C.

amount of excess xanthate in the reaction solution, and a new feature (B) at 256 nm originating from altered C–S bonding, and a broad maximum (D) at 420–430 nm attributed to S–Cu bonds, which produced the yellow color of the hydrosol, emerged. The transformations occurred in several seconds; afterward, the spectra changed very little until the precipitation of yellow copper xanthate, which typically occurred after a few hours, depending on the mixture composition and temperature.

TEM

Representative TEM micrographs (Fig. 2, see also ESI†) of the copper *n*-butyl xanthate colloids prepared with excess xanthate (Fig. 2a) demonstrate the formation of particles with diameters of 20–80 nm that tended to aggregate, at least upon drying the hydrosol, and were bridged, possibly with residual dixanthogen. Closer examination of the images (see inset) suggests that the nanoparticles were constructed of a denser core and a shell with a thickness of 5–10 nm. Broad diffuse rings were observed in the selected area electron diffraction (SAED) pattern at approximately 0.12 nm and 0.2–0.25 nm; the first value is close to the typical interatomic C–O and C–S distances in xanthate anion, and the second one is typical of the alkyl chain length and Cu–S bond distance.[3,26] In general, the electron diffraction patterns are indicative of poorly crystalline or amorphous particle structures. The products formed at xanthate-to-Cu ratios of approximately 2 and smaller (Fig. 2b) are primarily composed of 100–200 nm aggregates of densely packed nanoparticles surrounded by unstructured matter; the latter easily decomposed under electron beam (Fig. 2c), yielding 3–5 nm nanocrystals (SAED rings at 0.33 nm, 0.23 nm, 0.17 nm, *etc.*), which may be attributed to

hexagonal chalcocite (Cu_2S) (JCPDS no. 26-1116). For comparison, precipitates from more concentrated solutions consist mainly of irregular 200–400 nm particles (Fig. 2d). Similar TEM data were also obtained for other xanthates.

DLS and zeta-potential studies

Fig. 3 shows the average hydrodynamic diameters (Z_{av}) and zeta-potentials of the reaction products for various xanthates after 15 min of reaction as functions of their concentration. The particle size was about 120 nm in media with ROCSSK-to-$CuSO_4$ molar ratios lower than 2. Particle size was maximized at the xanthate-to-copper ratio of 2 and then fell to less than 100 nm when excessive xanthate was added. These dimensions are in reasonable accord with those observed using *ex situ* TEM. The zeta potentials were positive at reactant ratios ≤ 2 and sharply decreased with increasing xanthate content. This behavior concurs with the abovementioned reaction of Cu^{2+} ions with two xanthate molecules,[1–4,20–23] yielding copper xanthate and dixanthogen. The positive surface charges of the particles prepared using over-stoichiometric quantities of cupric ions seems to induce aggregation into (sub)micrometer entities, while excess xanthate anions result in negative nanoparticle surface charge and smaller hydrodynamic size. Generally, xanthates with shorter alkyl chains exhibit lower zeta-potential magnitudes and form larger particles, especially in media containing excess copper; however, the situation is not straightforward at xanthate-to-copper ratios above 2. Interestingly, the largest particles were obtained with ethyl xanthate. The mechanisms behind these phenomena are not entirely clear; the effects of impurities remaining after xanthate purification or/and formed due to reagent decomposition[1–4,22] cannot be ruled out. It is worth noting that somewhat different
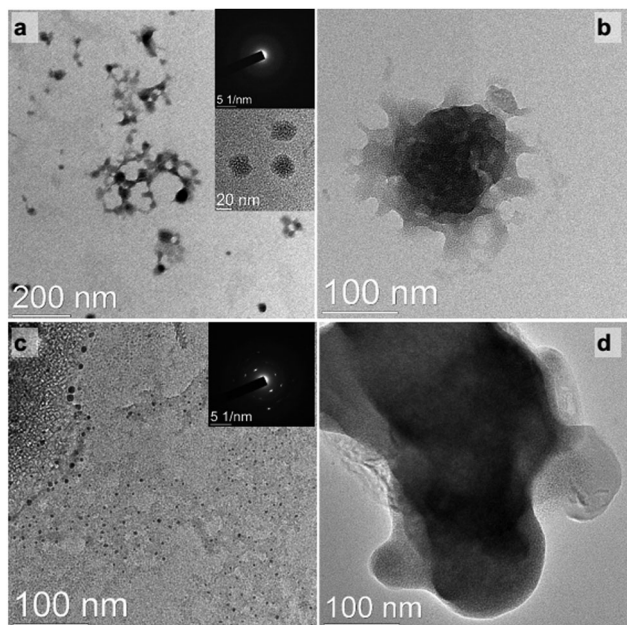

Fig. 2 Typical TEM micrographs and electron diffraction patterns of hydrosols prepared using the potassium *n*-butyl xanthate to $CuSO_4$ (1 mM) molar ratios of 4 (a) and 2 (b and c) at room temperature and (d) the sample precipitated from the 0.1 M solution.
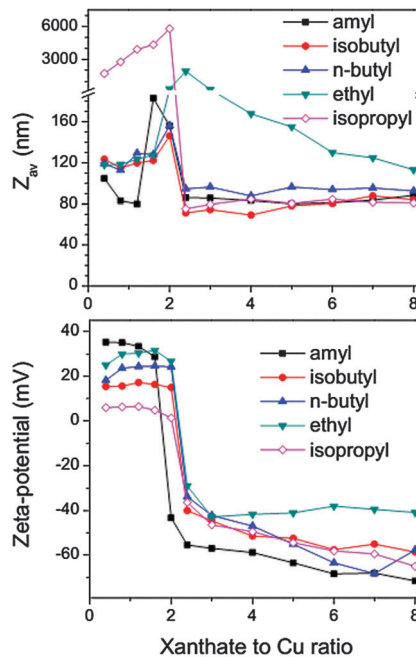

Fig. 3 Effect of molar reactant ratios on the hydrodynamic diameter and zeta potential of copper xanthates for xanthates with various alkyl chains after 15 min reaction (1 mM $CuSO_4$ 20 °C).

and less reproducible results (data not shown in the figures) were obtained in experiments with commercial xanthates, which were used as received; this should be taken into account when cheap commercial reagents are employed without additional purification, for example, in flotation practice.

The influences of reaction temperature and time on the particle size are illustrated in Fig. 4 for copper n-butyl xanthate. The particles were larger at higher temperatures, and the differences in the hydrodynamic diameter arose during the first seconds of the reaction. Usually, the effect of temperature was less pronounced when more xanthate was added, suggesting that the aggregation of nanoparticles was at least one of the reasons for the observable particle growth.

Thermogravimetry and FTIR

TGA of the copper n-butyl xanthate as an example (Fig. 5) showed that the sample separated by centrifugation lost $\sim$75 mass% at about 190 °C, and the sample subsequently treated with acetone for dixanthogen removal lost about 60 mass% at a higher temperature (about 200 °C). The main weight difference was due to the evaporation of about 15 mass% of the dixanthogen admixture at 160–170 °C, both in air and under inert atmosphere. The mass losses ($\sim$60% for copper butyl xanthates) are between those calculated for the decomposition to CuS (56.5%) and Cu_2S (63.8%). At the same time, the behavior of the samples between 250 °C and 900 °C, although somewhat different (ESI†), was characteristic of Cu_2S[33] but not covellite (CuS).[34] This disagrees with the previous works[17,32] that reported the formation of CuS and is worthy of further investigation.

The FTIR spectra (Fig. 6) of the samples obtained from solutions containing various concentrations and ratios of reagents, including those with excessive Cu^{2+} ions, were very similar, indicating that the particles had the same bulk compositions and structures; thus, their diverse behavior in solution (Fig. 3) was due to interfacial phenomena. The spectra of the copper xanthates along with dixanthogen and potassium xanthate as reference materials coincide with those reported by Little and co-workers.[21] The spectrum (c) of the sample treated with
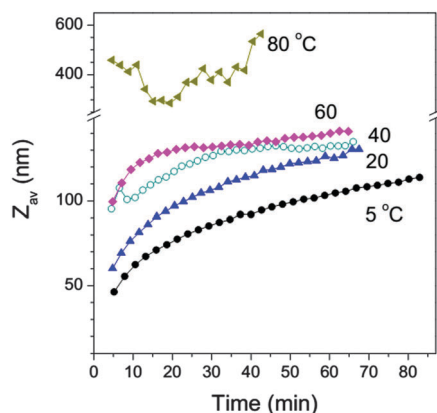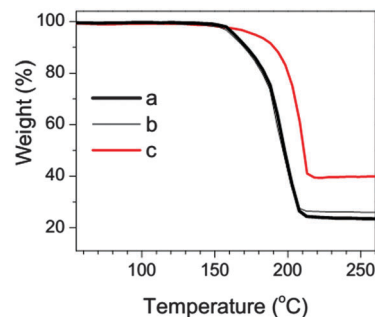
Fig. 5 TGA profiles of copper n-butyl xanthate (a and b) precipitated via centrifugation and (c) the sample treated with acetone to remove the admixture of dibutyl dixanthogen in air (a and c) and Ar (b) atmosphere.
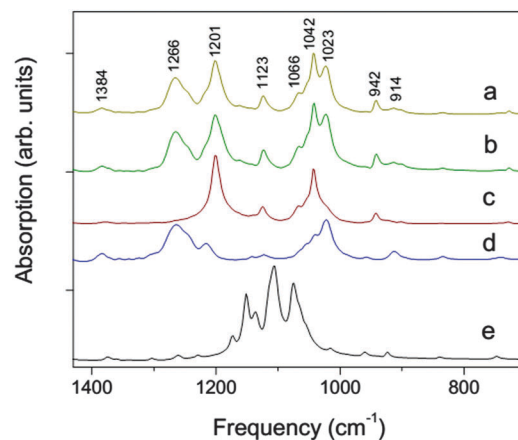
Fig. 6 FTIR spectra of (a) copper n-butyl xanthate prepared with xanthate-to-copper ratios of (a) 3 and (b) 1.5, (c) sample (a) washed with acetone, (d) sample (a) washed with dibutyl dixanthogen, and (e) sample (a) washed with potassium n-butyl xanthate.

acetone to remove dixanthogen can be described as the difference between the spectra of Cu xanthate (a, b) and dixanthogen (d), confirming the presence of the latter in the precipitated samples.

XPS and X-ray absorption spectroscopy

Dixanthogens evaporate in ultra-high vacuum, and concentrations measured by XPS (for copper n-butyl xanthate, at%: Cu 8.5, S 17, O 14.8, C 59.6) correspond to the Cu-to-S ratio of 1 to 2; some deviations from the ROCSSCu composition are due to an inevitable surface contamination by carbon and oxygen-bearing species. The Cu 2p spectra (Fig. 7) exhibits the Cu $2p_{3/2}$ peak at 932.9 eV, no shake-up satellites at 944–948 eV, and the Auger Cu L_3MM peak at 916 eV, indicating that copper occurs as Cu(I).[35–39] The S 2p band can be fitted using principal components with an S $2p_{3/2}$ binding energy of 162.3 eV and a minor one at 164.3 eV (about 5 relat%); the latter may be attributed to bridging sulfur atoms in residual dixanthogen[39,40] uptaken by the disordered cuprous xanthate. The C 1s spectrum diverges from that of potassium xanthate, which contains the lines of aliphatic carbon at 285.0 eV and equal intensity of the bands at about 286.5 eV (R–C–O–) and 288 eV (–O–C–SS–).[39,40] The discrepancy may be due to the xanthate

Fig. 4 Time evolution of the hydrodynamic diameter of copper n-butyl xanthate nanoparticles (initial xanthate-to-copper molar ratio = 4) at various temperatures.
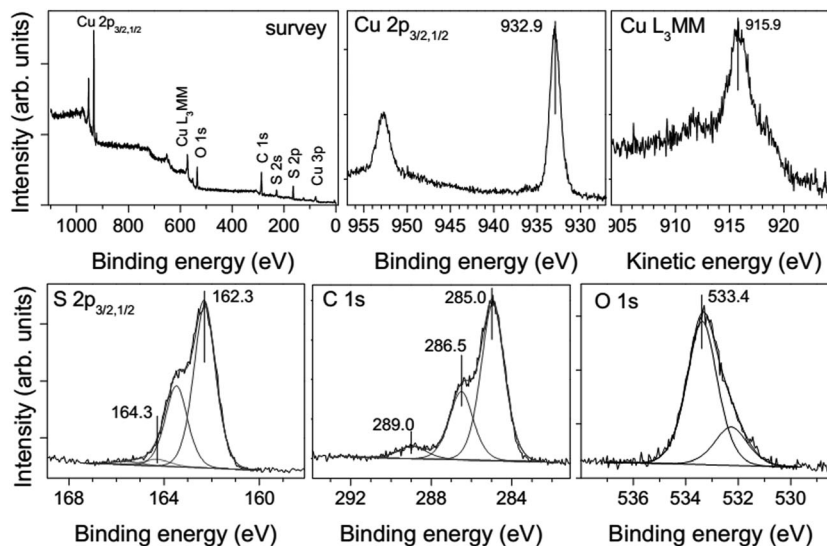
Fig. 7 X-ray photoelectron spectra of copper *n*-butyl xanthate.

radicals oriented outward from the surface, adsorption of products (particularly butanol) of xanthate and copper xanthate surface oxidation and decomposition in water and in vacuum under X-ray irradiation and of carbon contaminants. Akin to the FTIR spectra, the XPS spectra acquired from the samples prepared with an excess or deficit of xanthate and at various reagent concentrations were very similar, and, on the whole, agreed with those reported previously for cuprous xanthates.[6,36,39]

Fig. 8 shows the S K-edge and Cu K-edge XANES spectra measured in both the surface-sensitive TEY mode, which are noisy because of the poor conductivity of the material, and in the FY mode, which has a larger probing depth. The TEY and FY spectra of sulfur are rather similar, with two absorption peaks at 2470 and 2471.7 eV attributable to electron transitions from S 1s to σ* S–Cu states and S–C states with p-character, respectively.[41–43] A bump at about 2480 eV originates from oxidized surface sulfur species (*e.g.*, sulfate). In contrast, the Cu K-edge XANES spectra in the TEY and FL modes and thereby the states of copper in the near-surface layer and in the particle bulk clearly differ, with the FY spectrum being close to the Cu K-XANES spectrum of cuprous xanthate reported by Pattrick *et al.*[36] Based on earlier spectroscopic studies,[35,36,44–47] we can conclude that the Cu atoms in the core are four-fold coordinated

to S and bear a lower positive charge, while the coordination number of copper(I) within the shell is smaller and has a larger local charge. This agrees with previous studies on crystalline binary copper xanthates,[26,48,49] in which the copper atom was reported to exist either in a distorted tetrahedral S_4 environment[48] or in CuS_3 units.[49] Further studies are necessary to elucidate these disordered structures.

Factors affecting the characteristics of the colloids

The direct interaction between cupric ions and various xanthates in aqueous solution without capping agents or additional reagents produces copper xanthate colloids, which are stable at the copper concentrations less than 10 mM. The surface properties, colloidal stability and morphology of the particles greatly depend on the initial copper-to-xanthate ratio, with the colloids being more stable for excess xanthate, lower temperature and longer alkyl chain, although the effect of the latter factor is less obvious. The lower solubilities in water of copper xanthates and dixanthogens with larger alkyl groups[23] and, probably, the smaller concentrations of impurities seem to improve the hydrosol stability. It should be noted that the nature of the alkyl chain strongly affects the hydrophobicity (and floatability) of minerals with xanthate adsorbed on their surfaces,[5,6,23] the thermal decomposition of solid metal xanthates,[15–19] and so on; however, these phenomena still need to be studied in colloids and immobilized nanoparticles.

It is also necessary to take into consideration that dixanthogen, which is another poorly water-soluble reaction product, forms negatively charged nanodroplets (to be published in detail elsewhere). The species could interact more strongly with positively charged copper xanthate particles in media containing excessive copper ions than with negatively charged ones in the presence of excess xanthate anions. Dixanthogen partially co-precipitates with copper xanthate, covering and bridging the nanoparticles and affecting their properties. A few percent dixanthogen may be incorporated in the copper xanthate particles, disordering their structures. It is particularly interesting that the copper butyl
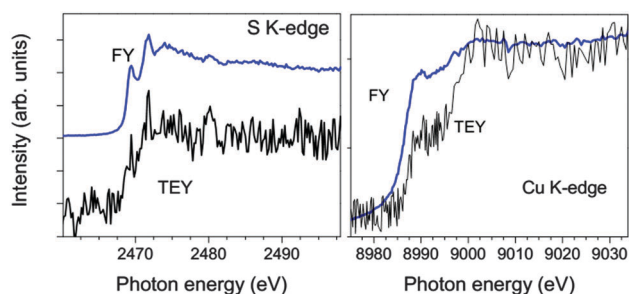

Fig. 8 X-ray absorption S–K and Cu K-XANES spectra collected in TEY and fluorescence yield modes from copper *n*-butyl xanthate precipitate.

xanthate precipitate containing some dixanthogen decomposes at a lower temperature than it does after the extraction of dixanthogen.

The phenomena and species described above should play a role in the transport of copper xanthates in the environment, technological and biological media. The findings should be taken into account or implemented in several fields, including flotation practice, water treatment, and the manufacturing of copper xanthate and copper sulfide nanostructures.

Conclusions

Colloidal copper(ı) xanthate nanoparticles having the composition ROCSSCu (R = ethyl, isopropyl, butyl, amyl groups) and diameters of 20–80 nm were formed by mixing aqueous solutions of cupric sulfate and potassium xanthates; the rapid appearance of a maximum at about 430 nm in the UV-vis absorption spectra indicated that the chemical reaction was largely completed in less than 1 min. A sharp change in the zeta potential and hydrodynamic diameter of the particles occurred at the xanthate-to-cupric ion molar ratio of 2, corresponding to the stoichiometric reaction. The particles produced at high xanthate concentrations had a high magnitude of negative zeta potential and lower diameter and higher stability than the positively charged particles formed with excess cupric ions. Smaller particles emerged at lower temperatures. IR spectroscopy and TGA demonstrated that the precipitated material comprised dixanthogen (on the order of 15 mass% for butyl xanthates), which likely promoted the aggregation of colloidal copper xanthate, especially in the solutions with excess copper ions. The admixture of dixanthogen also decreased the temperature of thermal decomposition of the precipitates, likely yielding chalcocite (Cu_2S) nanoparticles. SAED, FTIR, and XPS analysis revealed disordered structures and very similar compositions for copper xanthates prepared using various concentrations and ratios of reagents. At the same time, the TEM images and S K- and Cu K-edge XANES spectra collected in TEY and FY modes suggested a core/shell particle structure. The results are important for understanding the behavior of copper xanthates in several technological media and for further fine-tuning their properties for specific applications.

Acknowledgements

References

1 S. R. Rao, *Xanthate and Related Compounds*, Marcel Dekker, New York, 1971.
2 G. Winter, *Rev. Inorg. Chem.*, 1980, **2**, 253.
3 E. R. T. Tiekink and G. Winter, *Rev. Inorg. Chem.*, 1992, **12**, 183.
4 G. H. Harrison, Xanthates. in *Kirk-Othmer Encyclopedia of Chemical Technology*, ed. M. Howe-Grant, John Wiley & Sons, New York, 1998, pp. 713–734.
5 S. M. Bulatovic, *Handbook of Flotation Reagents-Chemistry, Theory and Practices, vol. 1 – Flotation of sulfides ores*, Elsevier, Amsterdam, 2007.
6 A. P. Chandra, L. Puskar, D. J. Simpson and A. R. Gerson, *Int. J. Miner. Process.*, 2012, **114–117**, 16.
7 Y.-K. Chang, J.-E. Chang, T.-T. Lin and Y.-M. Hsu, *J. Hazard. Mater.*, 2002, **B94**, 89.
8 S. Chakraborty and V. Tare, *Bioresour. Technol.*, 2006, **97**, 2407.
9 M. R. Mahmoud, N. K. Lazaridis and K. A. Matis, *Process Saf. Environ. Prot.*, 2015, **94**, 203.
10 W. Friebolin, G. Schilling, M. Zöller and E. Amtmann, *J. Med. Chem.*, 2004, **47**, 2256.
11 W. Friebolin, G. Schilling, M. Zöller and E. Amtmann, *J. Med. Chem.*, 2005, **48**, 7925.
12 S. Efrima and N. Pradhan, *C. R. Chim.*, 2003, **6**, 1035.
13 H. J. Moore, R. Colorado Jr., H. J. Lee, A. C. Jamison and T. R. Lee, *Langmuir*, 2013, **29**, 10674.
14 N. Pradhan, B. Katz and S. Efrima, *J. Phys. Chem. B*, 2003, **107**, 13843.
15 H. C. Leventis, S. P. King, A. Sudlow, M. S. Hill, K. C. Molloy and S. A. Haque, *Nano Lett.*, 2010, **10**, 1253.
16 T. Rath, C. Padeste, M. Vockenhuber, C. Fradler, M. Edler, A. Reichmann, I. Letofsky-Papst, F. Hofer, Y. Ekinci and T. Griesser, *J. Mater. Chem. A*, 2013, **1**, 11135.
17 A. Rabkin, O. Friedman and Y. Golan, *J. Colloid Interface Sci.*, 2015, **457**, 43.
18 E. A. Lewis, P. D. McNaughter, Z. Yin, Y. Chen, J. R. Brent, S. A. Saah, J. Raftery, J. A. M. Awudza, M. A. Malik, P. O'Brien and S. J. Haigh, *Chem. Mater.*, 2015, **27**, 2127.
19 A. Fischereder, A. Schenk, T. Rath, W. Haas, S. Delbos, C. Gougaud, N. Naghavi, A. Pateter, R. Saf, D. Schenk, M. Edler, K. Bohnemann, A. Reichmann, B. Chernev, F. Hofer and G. Trimme, *Monatsh. Chem.*, 2013, **144**, 273.
20 M. P. Matuszak, *J. Am. Chem. Soc.*, 1931, **53**, 4451.
21 G. H. Little, G. W. Poling and J. Leja, *Can. J. Chem.*, 1961, **39**, 745.
22 N. Sheikh, *The chemical stability of heavy metal xanthates*, PhD thesis, Univ. British Columbia, 1972.
23 P. K. Ackerman, G. H. Harris, R. R. Klimpel and F. F. Aplan, *Int. J. Miner. Process.*, 1987, **21**, 141.
24 R. Woods, G. A. Hopes and G. M. Brown, *Colloids Surf., A*, 1998, **137**, 329.
25 S. S. Garje and V. K. Jain, *Coord. Chem. Rev.*, 2003, **236**, 35.
26 E. R. T. Tiekink and I. Haiduc, *Prog. Inorg. Chem.*, 2005, **54**, 127.
27 A. O. Görgülü, M. Arslan and E. Çil, *J. Coord. Chem.*, 2006, **59**, 1913.
28 P. Hellstrom, S. Oberg, A. Fredriksson and A. Holmgren, *Spectrochim. Acta*, 2006, **65A**, 887.
29 D. Rusanova, K. E. Christensen, I. Persson, K. J. Pike, O. N. Antzutkin, X. Zou, R. Dupree and W. Forsling, *J. Coord. Chem.*, 2007, **60**, 517.
30 B. Bag, B. Das and B. K. Mishra, *Miner. Eng.*, 2011, **24**, 760.
31 L. C. Juncal, Y. A. Tobón, O. E. Piro, C. O. Della Vėdova and R. M. Romano, *New J. Chem.*, 2014, **38**, 3708.

32 T. C. Vagvala, S. S. Pandey, Y. Ogomi, T. Ma and S. Hayase, *Inorg. Chim. Acta*, 2015, **435**, 292.

33 J. G. Dunn, A. R. Ginting and B. O'Connor, *J. Therm. Anal.*, 1994, **41**, 671.

34 J. G. Dunn and C. Muzenda, *Thermochim. Acta*, 2001, **369**, 117.

35 R. A. D. Pattrick, J. F. W. Mosselmans, J. M. Charnock, K. E. R. England, G. R. Helz, C. D. Garner and D. J. Vaughan, *Geochim. Cosmochim. Acta*, 1997, **61**, 2023.

36 R. A. D. Pattrick, K. E. R. England, J. M. Charnock and J. F. W. Mosselmans, *Int. J. Miner. Process.*, 1999, **55**, 247.

37 S. W. Goh, A. N. Buckley, W. M. Skinner and L.-J. Fan, *Phys. Chem. Miner.*, 2010, **37**, 389.

38 S. Saikova, S. Vorobyev, M. Likhatski, A. Romanchenko, S. Erenburg, S. Trubina and Y. Mikhlin, *Appl. Surf. Sci.*, 2012, **258**, 8214.

39 A. V. Shchukarev, T. O. Nichiporenko and G. N. Mashevskiy, *Obogashch. Rud*, 1992, **1**, 21, in Russian.

40 I. Kartio, K. Laajalehto, E. Suoninen, S. Karthe and R. Szargan, *Surf. Interface Anal.*, 1992, **18**, 807; R. Szargan, S. Karthe and E. Suoninen, *Appl. Surf. Sci.*, 1992, **55**, 227.

41 D. Li, G. M. Bancroft, M. Kasrai, M. E. Fleet, X. H. Feng, B. X. Yang and K. H. Tan, *Phys. Chem. Miner.*, 1994, **21**, 317.

42 R. Chauvistré, J. Hormes, E. Hartmann, N. Etzenbach, R. Hosch and J. Hahn, *Chem. Phys.*, 1997, **223**, 293.

43 T. Tsuduki, A. Imanishi, K. Isawa, S. Terada, F. Matsui, M. Kiguchi, T. Yokoyama and T. Ohta, *J. Synchrotron Radiat.*, 1999, **6**, 787.

44 L.-S. Kau, D. J. Spira-Solomon, J. E. Penner-Hahn, K. O. Hodgson and E. I. Solomon, *J. Am. Chem. Soc.*, 1987, **109**, 6433.

45 J. R. Vegelius, K. O. Kvashnina, H. Hollmark, M. Klintenberg, Y. O. Kvashnin, I. L. Soroka, L. Werme and S. M. Butorin, *J. Phys. Chem. C*, 2012, **116**, 22293.

46 P. Kumar, R. Nagarajan and R. Sarangi, *J. Mater. Chem. C*, 2013, **1**, 2448.

47 A. S. Jullien, C. Gateau, I. Kieffer, D. Testemale and P. Delangle, *Inorg. Chem.*, 2013, **52**, 9954.

48 K. Tang, X. Jin, Y. Long, P. Cui and Y. Tang, *J. Chem. Res., Synop.*, 2000, **2000**, 452.

49 C. Wycliff, D. S. Bharathi, A. G Samuelson and M. Nethaji, *Polyhedron*, 1999, **18**, 949.